

See discussions, stats, and author profiles for this publication at: <https://www.researchgate.net/publication/224083669>

# Fractal growth in organic thin films: Experiments and modeling

ARTICLE *in* APPLIED PHYSICS LETTERS · DECEMBER 2009

Impact Factor: 3.3 · DOI: 10.1063/1.3238316 · Source: IEEE Xplore

---

CITATIONS

11

---

READS

47

4 AUTHORS, INCLUDING:



**Richard H. Gee**

Lawrence Livermore National Laboratory

86 PUBLICATIONS 1,207 CITATIONS

SEE PROFILE



**Amitesh Maiti**

Lawrence Livermore National Laboratory

155 PUBLICATIONS 4,601 CITATIONS

SEE PROFILE

# Fractal growth in organic thin films: Experiments and modeling

Gengxin Zhang,<sup>1</sup> Brandon Weeks,<sup>1,2,a)</sup> Richard Gee,<sup>3</sup> and Amitesh Maiti<sup>3,b)</sup>

<sup>1</sup>Department of Chemical Engineering, Texas Tech University, Lubbock, Texas 79409, USA

<sup>2</sup>Department of Chemistry and Biochemistry, Texas Tech University, Lubbock, Texas 79409, USA

<sup>3</sup>Lawrence Livermore National Laboratory, Livermore, California 94451, USA

(Received 24 June 2009; accepted 7 September 2009; published online 16 November 2009)

Optical microscopy and atomic force microscopy were used to investigate the solidification process of the organic energetic material pentaerythritol tetranitrate thermally deposited on a silicon surface. The metastable films spontaneously undergo dendrite formation where the measured fractal dimensions indicate a diffusion-limited-aggregation mechanism. The branch growth rate was investigated as a function of temperature and fitted by a theoretical model that takes into account competing thermally activated processes of surface diffusion and molecular desorption. Consideration of the internal molecular degrees of freedom is shown to be essential for quantitative consistency between theory and experiment. © 2009 American Institute of Physics.

[doi:10.1063/1.3238316]

The physics of thin organic film growth is an intriguing and important topic in nonequilibrium solidification process.<sup>1,2</sup> Examples of such processes include nonequilibrium pattern formation,<sup>3</sup> dendrite growth,<sup>2</sup> and viscous fingering.<sup>4</sup> A number of growth and aggregation models have been developed to explain the physical and chemical characteristics including diffusion limited aggregation (DLA),<sup>5</sup> cluster-cluster aggregation,<sup>6</sup> and deposition diffusion and aggregation.<sup>7</sup> These models have been used for both metal<sup>8,9</sup> and inorganic<sup>10</sup> thin films. The majority of studies have considered metallic systems where aggregation and desorption involve individual metal atoms. Expanding these models to a molecular system would be interesting due to the additional internal degrees of freedom of individual molecules that strongly affect their kinetics. In addition, molecular thin films are important in many areas including pharmaceuticals,<sup>11</sup> paints/pigments, agrochemicals,<sup>12</sup> and energetic materials.<sup>13</sup>

In this letter, we report the investigation of fractal growth of pentaerythritol tetranitrate (PETN) films thermally deposited on a silicon substrate. At room temperature, the island growth clearly exhibits dendrite shapes with fractal dimensions typical of a DLA process. We develop a simple theoretical model to show how such patterns can be explained on the basis of competing effects of diffusion-mediated aggregation and desorption of molecules.

PETN (purity > 99%) supplied by Lawrence Livermore National Laboratory (LLNL) was used in these experiments without further purification. Electronic-grade silicon wafers (Nova Electronic Materials, Ltd.) were cleaned by a routine procedure.<sup>14</sup> PETN films were deposited with thermal deposition chamber,<sup>15</sup> which has *in situ* temperature and thickness measurement capability. A Maxtek T-100 QCM film thickness monitor was used to check the flux and film thickness. The as-deposited PETN films, ranged from 10 to 1000 nm in thickness, were annealed at temperatures ranging from 30 and 80 °C, while the film growth process was monitored by

optical microscopy. All atomic force microscopy (AFM) images were collected using a Nanoscope IIIa multimode scanning probe microscope (Veeco Instruments, Inc., Santa Barbara, CA) operating in the tapping mode using a silicon cantilever with a nominal drive frequency of 325 kHz.

AFM images of the freshly prepared PETN films appear to follow the Volmer–Weber structure<sup>16</sup> with island structures, as shown in Fig. 1. PETN is easily supercooled to room temperature without crystallization [melting point of  $141 \pm 1$  °C (Ref. 17)]. The nucleation rate of islands appears to be homogeneous over the entire surface. The initial films prepared are metastable over a period of days, showing no dendritic growth. Previous studies showed that by inducing defects on the surface with the AFM tip, PETN films spontaneously undergo dendritic formation.<sup>18</sup> However, that work was primarily phenomenological and there was no effort to deduce the mechanisms responsible for the fractal growth. Figure 2 shows clear observation of branch formation at four subsequent time elapses after initiation of dendrite growth.

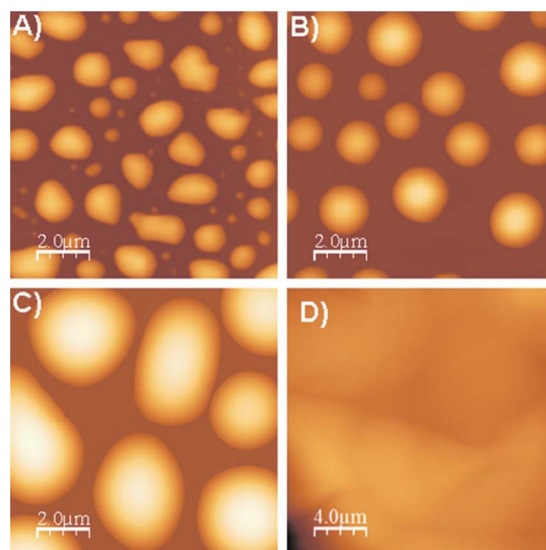


FIG. 1. (Color online) AFM images of PETN films deposited on silicon. The film thicknesses measured by QCM are (a) 40.2 nm, (b) 70 nm, (c) 280.2 nm, and (d) ~500 nm.

<sup>a)</sup> Author to whom correspondence should be addressed. Electronic mail: brandon.weeks@ttu.edu.

<sup>b)</sup> Electronic mail: amaiti@llnl.gov.

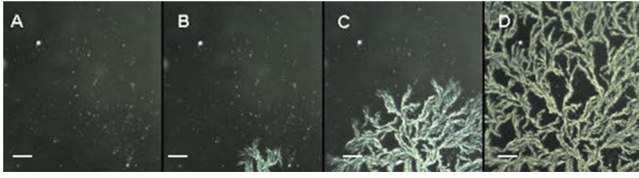


FIG. 2. (Color online) Optical images of PETN deposited on silicon showing dendritic growth at room temperature. (a) As deposited PETN, (b) Image after 60 min, (c) 90 min, and (d) after 170 min. The scale bar is 100  $\mu\text{m}$ .

The formation of dendritic branches is found to occur at the expense of island shrinkage. The termination of growth results from the depletion of material surrounding the branches, and the fractal shapes are stable when the branches are fully developed, as shown in Fig. 2.

The temperature of the environment is found to influence the growth rate of the branches. To quantify the effect of the temperature, we measured the average branch growth rate during annealing (Fig. 3). At 30  $^{\circ}\text{C}$  the rate of growth is found to be 0.15 ( $\pm 0.03$ )  $\mu\text{m/s}$ . The growth rate increases almost linearly and displays an interesting maximum at  $\sim 45$   $^{\circ}\text{C}$  before falling to essentially zero at 60  $^{\circ}\text{C}$ . Further heating led to shrinkage of the dendrite structures with complete disappearance at 85  $^{\circ}\text{C}$ .

The rates of growth and shrinkage of the dendritic branches as a function of temperature can be understood within the framework of a simple theoretical model that takes into account competing processes of (1) surface-diffusion-mediated molecular aggregation and (2) thermal desorption of PETN molecules from the aggregated dendrites. Process (1) dominates at temperatures less than 60  $^{\circ}\text{C}$ , thereby leading to a net growth rate of the branches, while process (2) takes over at higher temperatures, resulting in feature shrinkage and ultimate disappearance. The model is mathematically described as below.

A dendrite with linear dimensions  $s$  and fractal dimension  $f$  consists of a total number of molecules given by  $N(s) = ks^f$ , where  $k$  is a proportionality constant. The rate of molecular addition to this dendrite is given by

$$\dot{N}_+ = p_d A(s) \nu \exp(-\Delta_+/k_B T), \quad (1)$$

where a “dot” represents the time rate of change (everywhere throughout the text),  $\Delta_+ = \Delta_{\text{gen}} + \Delta_{\text{diff}}$  is the sum of (1) the

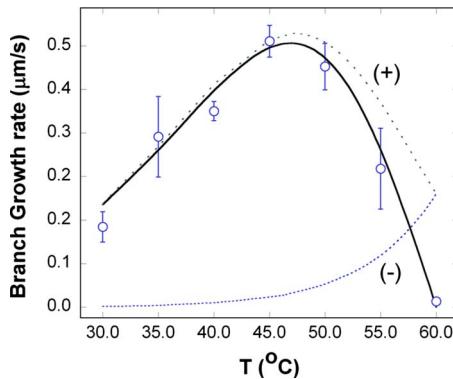


FIG. 3. (Color online) Growth rate of dendrite branches as a function of temperature. Circles indicate experimental observations. The solid line represents the theoretical net growth curve; it is a sum of the dotted (+) and dashed (−) curves showing the addition rate by diffusion and the reduction rate through evaporation, respectively.

activation barrier of the generation of the surface-mobile molecules from the amorphous film surface ( $\Delta_{\text{gen}}$ ) and (2) the activation barrier of surface diffusion of the mobile species ( $\Delta_{\text{diff}}$ ), while  $A(s)$  contains unknowns such as the prefactor of diffusion constant, prefactor of surface density of mobile species, etc., but should be relatively insensitive to temperature  $T$ , which is already expressed through the exponential term. The quantity  $\nu$  in Eq. (1) is an effective vibrational frequency and  $p_d$  is the probability that the diffusing molecule does not desorb from the surface during its diffusion path to the dendrite. This probability is given by  $p_d = \exp(-r_d \tau_d)$ , where  $r_d$  is the rate of desorption (into the vacuum) from the diffusing surface and  $\tau_d$  is the average diffusion time. These quantities can be estimated as  $r_d \sim \nu \exp(-\Delta_{\text{des}}/k_B T)$  and  $\tau_d \sim (\lambda_d^2/a^2 \nu) \exp(\Delta_{\text{diff}}/k_B T)$ , where  $\Delta_{\text{des}}$  is the energy barrier to desorb from the diffusing surface,  $\lambda_d$  is a mean-free path of diffusion, and  $a$  is the nearest-neighbor distance on the Si surface, being  $\sim 0.5$  nm.

While  $\dot{N}_+$  represents a source term, there is a sink term that is governed by the thermal desorption of PETN molecules<sup>19,20</sup> from the dendrite, which is given by the expression  $\dot{N}_- = (P_{\text{eq}}/\sqrt{2\pi M k_B T}) \alpha N_{\text{surf}}(s)$ , where  $N_{\text{surf}}(s)$  is the number of surface-exposed sites of the dendrite,  $M$  and  $\alpha$  are the mass and the surface area per PETN molecule, and  $P_{\text{eq}}$  is the equilibrium pressure given by the formula,<sup>19</sup>

$$P_{\text{eq}} = \frac{k_B T}{\Lambda^3} \frac{Z_{\text{rot}}}{\{Z_{\text{vib}}(\nu_{\text{eff}})\}^6} \exp(-\Delta E_{\text{sub}}/k_B T), \quad (2)$$

where  $Z_{\text{rot}}$  and  $Z_{\text{vib}}$  are rotational and vibrational partition functions of a PETN molecule,<sup>19</sup>  $\Lambda$  is the thermal de Broglie wavelength ( $\Lambda = h/\sqrt{2\pi M k_B T}$ , with  $h$  being the Planck's constant),  $\nu_{\text{eff}} \sim 1.0 \times 10^{13} \text{ s}^{-1}$  is an effective frequency defined in Ref. 19 that accurately reproduces PETN vapor pressure, and  $\Delta E_{\text{sub}}$  is the sublimation energy. The experimentally observed “branch growth rate” is simply the rate of change in  $s$ . This is given by the equation,  $\dot{N}_s = \dot{N}_+ - \dot{N}_-$ , which can be simplified to

$$\dot{s} = s \{ C_+(s) p_d \nu \exp(-\Delta_+/k_B T) - C_-(s) \dot{\phi}_{\text{des}} \}, \quad (3)$$

where  $C_+(s) = A(s)/[fN(s)]$  and  $C_-(s) = N_{\text{surf}}(s)/[fN(s)]$  are dimensionless quantities assumed insensitive to  $T$ , and the site desorption rate  $\dot{\phi}_{\text{des}}$  is given by

$$\dot{\phi}_{\text{des}} = \frac{k_B T}{h} \frac{\alpha}{\Lambda^2} \frac{Z_{\text{rot}}}{\{Z_{\text{vib}}(\nu_{\text{eff}})\}^6} \exp(-\Delta E_{\text{sub}}/k_B T), \quad (4)$$

a familiar expression from transition state theory.<sup>21</sup>

We now use the above formalism to interpret the observed branch growth rate in Fig. 3 for a fixed size scale  $s \sim 100 \mu\text{m}$  (see Fig. 2). From molecular dynamics calculations using the COMPASS force field,<sup>22</sup> we determined the relevant energies (in kcal/mol) as  $\Delta_{\text{gen}} \sim 22$ ,  $\Delta_{\text{diff}} \sim 2$ ,  $\Delta_{\text{des}} \sim 17$ , and  $\Delta E_{\text{sub}} \sim 37$ . We also assume all vibrational frequencies to be  $\nu \sim \nu_{\text{eff}} = 1 \times 10^{13} \text{ s}^{-1}$ . From Fig. 2 the diffusion mean-free path  $\lambda_d$  appears to be a few tens of microns. The solid curve in Fig. 3 displays the branch growth rate  $\dot{s}$  computed by Eq. (3) using parameters  $\lambda_d \sim 85 \mu\text{m}$ ,  $C_+(s) \sim 58.3$ , and  $C_-(s) \sim 5.2 \times 10^{-4}$ . The dotted (+) and dashed (−) curves also separately show the contribution of the source (i.e., addition rate by diffusion) and the sink (i.e., reduction rate through evaporation) terms to the overall growth process. The net growth rate is the difference be-

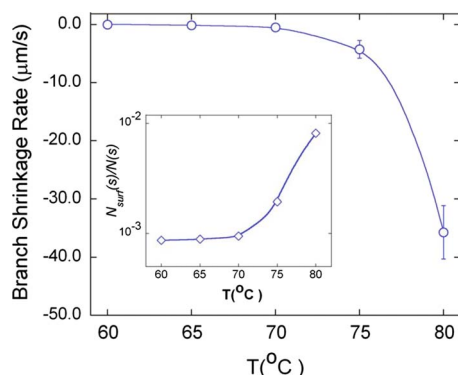


FIG. 4. (Color online) The experimental measurements (circles) of branch shrinking rate between temperatures of 60 and 80 °C, along with the corresponding theoretical fit (solid line). (Inset) Temperature-dependent surface fraction  $N_{\text{surf}}(s)/N(s)$  of molecules used in the theoretical fit.

tween the (+) and (−) curves. One clearly sees that the maximum at  $T \sim 45$  °C occurs solely in the source term. This is because this term involves the product of two functions [see Eq. (1)], i.e., the probability  $p_d$  that decreases as a function of  $T$  and  $\exp(-\Delta_+/k_B T)$  that increases as a function of  $T$ . Below 45 °C, the increase in growth rate with temperature is due to faster diffusion, which outweighs losses due to evaporation of the diffusing species. However, above 45 °C, the rate of evaporation of the diffusing species becomes too significant and leads to a gradual reduction in the growth rate. At the same time, the rate of evaporation from the dendrite surface picks up beyond 45 °C and continues to increase. There is a crossover of the source and the sink contributions at 60 °C, leading to zero growth rate at this temperature and a net shrinking of the dendrite beyond 60 °C. Figure 4 displays the experimentally measured branch shrinking rate between temperatures of 60 and 80 °C. If we use a constant value of the surface fraction  $N_{\text{surf}}(s)/N(s)$  [which is just  $f$  times  $C_-(s)$ ] during the whole shrinking process, we get good agreement with the experimental shrinking rates for  $T$  up to 70 °C. However, for higher temperatures, we find that the computed shrinking rates are progressively more underestimated. This can be interpreted as more and more sites being surface exposed at higher temperatures with a concomitant increase in surface fraction (see inset in Fig. 4).

In this work, we demonstrated dendrite growth from thin films of the energetic organic material PETN and quantitatively studied growth and shrinkage rates as a function of temperature. We showed that a simple theoretical model based on surface diffusion, aggregation, and thermal desorp-

tion can quantitatively explain the observed data provided internal molecular degrees of freedom are consistently incorporated in the desorption analysis. This work may aid in understanding growth kinetics and coarsening processes in PETN and other organic materials.

The authors would like to thank financial support from NSF CAREER (Grant No. CBET-0644832). The work at LLNL was performed under the auspices of the U.S. Department of Energy by Lawrence Livermore National Laboratory under Contract No. DE-AC52-07NA27344.

- <sup>1</sup>L. Granasy, T. Pusztai, T. Borzsonyi, J. A. Warren, and J. F. Douglas, *Nature Mater.* **3**, 645 (2004).
- <sup>2</sup>F. J. M. Z. Heringdorf, M. C. Reuter, and R. M. Tromp, *Nature (London)* **412**, 517 (2001).
- <sup>3</sup>V. Ferreiro, J. F. Douglas, J. A. Warren, and A. Karim, *Phys. Rev. E* **65**, 042802 (2002).
- <sup>4</sup>J. Nittmann, G. Daccord, and H. E. Stanley, *Nature (London)* **314**, 141 (1985).
- <sup>5</sup>T. A. Witten and L. M. Sander, *Phys. Rev. Lett.* **47**, 1400 (1981).
- <sup>6</sup>P. Meakin, *Phys. Rev. Lett.* **51**, 1119 (1983).
- <sup>7</sup>P. Jensen, A. L. Barabasi, H. Larralde, S. Havlin, and H. E. Stanley, *Phys. Rev. E* **50**, 618 (1994).
- <sup>8</sup>C. M. Feng, H. L. Ge, M. R. Tong, G. X. Ye, and Z. K. Jiao, *Thin Solid Films* **342**, 30 (1999).
- <sup>9</sup>D. Aurongzeb, E. Washington, M. Basavaraj, J. M. Berg, H. Temkin, and M. Holtz, *J. Appl. Phys.* **100**, 114320 (2006).
- <sup>10</sup>B. Blum, R. C. Salvarezza, and A. J. Arvia, *J. Vac. Sci. Technol. B* **17**, 2431 (1999).
- <sup>11</sup>C. S. Olsen and H. S. Scroggins, *J. Pharm. Sci.* **73**, 1303 (1984).
- <sup>12</sup>D. A. Knowles, *Chemistry and Technology of Agrochemical Formulations* (Springer, Berlin, 1998).
- <sup>13</sup>W. P. King, S. Saxena, B. A. Nelson, B. L. Weeks, and R. Pitchimani, *Nano Lett.* **6**, 2145 (2006).
- <sup>14</sup>The substrates were cleaned by Piranha solution (98%  $\text{H}_2\text{SO}_4$  and 30%  $\text{H}_2\text{O}_2$  in volume ratios of 3:1) under agitation for 30 min, rinsed with de-ionized water, and dried. Caution: piranha solution reacts violently with most organic materials and must be handled with extreme care.
- <sup>15</sup>G. Zhang, R. Pitchimani, and B. L. Weeks, *Rev. Sci. Instrum.* **79**, 096102 (2008).
- <sup>16</sup>M. Volmer and A. Weber, *Z. Phys. Chem.* **119**, 277 (1926).
- <sup>17</sup>N. W. Lam, J. E. Field, and H. M. Hauser, *J. Chem. Soc., Perkin Trans. 2* **1976**, 637.
- <sup>18</sup>G. Zhang and B. L. Weeks, *Scanning* **30**, 228 (2008).
- <sup>19</sup>A. Maiti, L. A. Zepeda-Ruiz, R. H. Gee, and A. K. Burnham, *J. Phys. Chem. B* **111**, 14290 (2007).
- <sup>20</sup>L. A. Zepeda-Ruiz, G. H. Gilmer, A. Maiti, R. H. Gee, and A. K. Burnham, *J. Cryst. Growth* **310**, 3812 (2008).
- <sup>21</sup>G. Hlawacek, P. Puschnig, P. Frank, A. Winkler, C. Ambrosch-Draxl, and C. Teichert, *Science* **321**, 108 (2008); S. Glasstone, K. J. Laidler, and H. Eyring, *The Theory of Rate Processes* (McGraw-Hill, New York, 1941); R. I. Masel, *Chemical Kinetics and Catalysis* (Wiley, New York, 2001).
- <sup>22</sup>S. W. Bunte and H. Sun, *J. Phys. Chem. B* **104**, 2477 (2000).